Chemistry Research Journal, 2021, 6(6):128-144

Available online www.chemrj.org

Research Article

ISSN: 2455-8990
CODEN(USA): CRJHA5

Quantum Chemical Analysis of the relationships between electronic structure and dopamine D_1 and D_5 receptor binding affinities in a series of 1-phenylbenzazepines

Juan S. Gómez-Jeria[1,2]*, Andrés Robles-Navarro[1], Valeria Soto-Martínez[1]

[1]Quantum Pharmacology Unit, Department of Chemistry, Faculty of Sciences, University of Chile. Las Palmeras 3425, Santiago 7800003, Chile
[2]Glowing Neurons Group, CP 8270745 Santiago, Chile
Corresponding author: facien03@uchile.cl

Abstract The Klopman-Peradejordi-Gómez QSAR equation was employed for searching formal quantitative relationships between the electronic structures of a group of 1-phenylbenzazepines and their affinities for the dopamine D_1 and D_5 receptors. The electronic structure was calculated with the Gaussian 16 software after a full geometry optimization. A linear multiple regression analysis was carried out by using the common skeleton approach and 20 local atomic reactivity indices per atom. Statistically significant relationships were found for both cases involving the local atomic properties of several atoms. For these atoms we have suggested possible interactions that could be tested by experimentalists using different substituents.

Keywords Dopamine, D_1 receptor, D_5 receptor, Klopman-Peradejordi-Gómez method, QSAR, receptor affinity, molecular interactions, Hartree-Fock local atomic reactivity indices, chemical reactivity

Introduction

Dopamine is a monoamine catecholamine neurotransmitter that binds to the dopamine receptors and has numerous different functions. There are five different dopamine receptors named D_1-D_5. Mishra, Singh and Shukla summarized the functions of these receptors [1]: The D_1 receptor is involved in locomotion, learning and memory, attention, impulse control, sleep and regulation of renal function. The D_2 receptor is involved in locomotion, learning and memory, attention, sleep and reproductive behaviour. The D_3 receptor is involved in locomotion, cognition, attention, impulse control, sleep and regulation of food intake. The D_4 receptor is involved in cognition, impulse control, attention, sleep and reproductive behavior. The D_5 receptor is involved in cognition, attention, decision making, motor learning and renin secretion [1]. They are divided in two categories.D_1 and D_5receptors belong to the D_1-like subfamily of G protein–coupled receptors that are coupled to G_s alpha subunit and mediate excitatory neurotransmission.D_2, D_3 and D_4 receptors constitute the D_2-like subfamily of G protein-coupled receptors that are coupled to G_i/G_o and mediate inhibitory neurotransmission.

The importance of these receptors has led to the synthesis and testing for dopamine receptors affinities of a large amount of molecules. In our laboratory we have analyzed the electronic determinants of the dopamine receptor affinity for several molecules and receptors [2-8]. Recently, Harding et al. reported the synthesis and dopamineD_1 and D_5 receptor affinities of a group of ring C ortho halogenated 1-phenylbenzazepines [9].

Here we report the first results of a quantum chemical search of formal quantitative relationships between electronic structure and the above reported affinities.

Methods, Models and Calculations

The Method

The Klopman-Peradejordi-Gómez QSAR equation was developed in several steps longtime ago. As it was fully reviewed, we present only the version employed in this study. The details can be found in the literature. It is a linear relationship involving local atomic reactivity indices of the atoms composing the molecule under study. Then, for any biological activity K we have [10-21]:

$$\log(K)=a+b\log\left(M_D\right)+\sum_{o=1}^{sub}\varphi_o+\sum_{i=1}^{Y}\left[e_iQ_i+f_iS_i^E+s_iS_i^N\right]+$$
$$+\sum_{i=1}^{Y}\sum_{m=(HOMO-2)^*,i}^{(HOMO)^*,i}\left[h_i\left(m\right)F_i(m^*)+j_i\left(m\right)S_i^E\left(m^*\right)\right]+$$
$$+\sum_{i=1}^{Y}\sum_{m'=(LUMO)^*,i}^{(LUMO+2)^*,i}\left[r_i\left(m'\right)F_i(m'^*)+t_i\left(m'\right)S_i^N\left(m'^*\right)\right]+$$
$$+\sum_{i=1}^{Y}\left[g_i\mu_i^*+k_i\eta_i^*+o_i\omega_i^*+z_i\zeta_i^*+w_jQ_i^{*,max}\right] \quad (1)$$

where K is a biological activity, M_D is the drug's mass and φ_o is the orientational parameter of the o-th substituent (the summation runs over all the substituents selected for the research). Q_i is the net charge of atom i and S_i^E and S_i^N are, respectively, the total atomic electrophilic and nucleophilic superdelocalizabilities of atom i. F_{i,m^*} is the electron population of atom i in occupied (empty) local MO m* (m'*), $S_i^E(m)^*$ is the orbital electrophilic superdelocalizability at occupied local MO m* of atom i and $S_i^N(m')^*$ is the orbital nucleophilic superdelocalizability at empty local MO m'* of atom i. μ_i^*, η_i^*, ω_i^*, ζ_i^* and $Q_i^{*,max}$ are, respectively, the local atomic electronic chemical potential, the local atomic hardness, the local atomic electrophilicity, the local atomic softness and the maximal amount of electronic charge that atom i may accept. These indices were developed within the Hartree-Fock formalism. The molecular orbitals with an asterisk are the Local Molecular Orbitals (LMO) of each atom. For atom x, the LMOs are defined as the subset of the molecule's MOs having an electron population greater than 0.01e on x. In this study we have considered the three highest occupied local MOs ((HOMO)*, (HOMO-1)*, (HOMO-2)*) and the three lowest empty local MOs ((LUMO)*, (LUMO+1)*, (LUMO+2)*) of each atom because experimental evidence indicates that they are determinant for molecular reactivity. The index Y in the summations runs over all atoms composing the molecule. Good results were obtained for different molecular systems and biological activities [22-38].

Selection of Molecules and Biological Activities

The selected molecules are a group of 1-phenylbenzazepinesselected from a recent study [9]. Their general formula and biological activity are displayed, respectively, in Fig. 1 and Table 1.

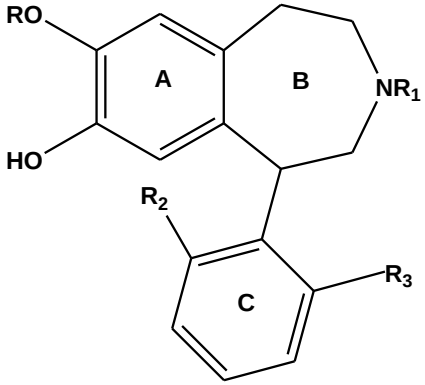

Figure 1: General formulas of 1-phenylbenzazepines

Table 1: 1-phenylbenzazepines and dopamine receptor affinities

Mol.	R	R_1	R_2	R_3	log(K) D_1	log(K) D_5
1	Me	H	H	H	2.1	2.49
2	Me	H	H	Cl	2.17	2.68
3	Me	H	Cl	Cl	1.88	1.4
4	Me	H	H	Br	1.86	1.91
5	H	H	H	Br	1.41	1.83
6	Me	Me	H	Cl	1.15	1.67
7	Me	Me	Cl	Cl	2.16	1.69
8	Me	Me	H	Br	1.2	1.67
9	Me	Allyl	H	Cl	1.68	2.42
10	Me	Allyl	Cl	Cl	3.02	2.68
11	Me	Allyl	H	Br	1.61	2.69
12	H	Me	H	Br	1.77	2.35
13	H	Allyl	H	Br	2.12	2.65

Figure 2 shows the histogram of frequencies for log(K) D_1 data [39]

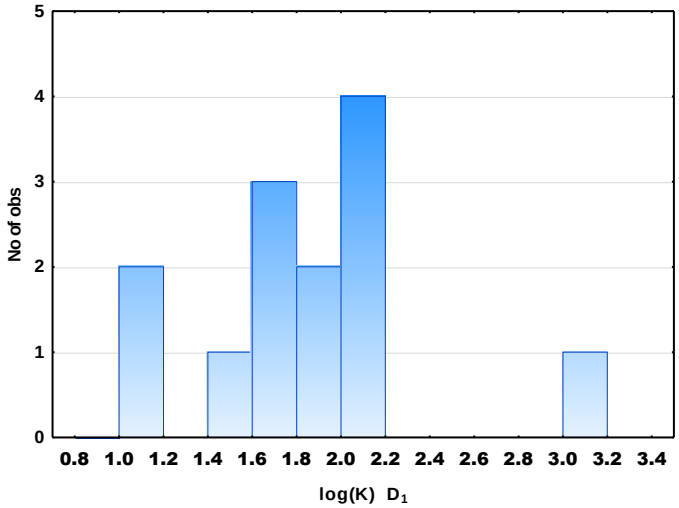

Figure 2: Histogram of frequencies for log(K) D_1 data

We can see that that the experimentalists obtained experimental D_1 data spanning about two orders of magnitude but with an empty interval between the values of log(K) 2.2 and 3. This fact is appreciated better in the next plot. Figure 3 shows the Box-Whiskers plot of log(K) D_1 values with median and quartile values.

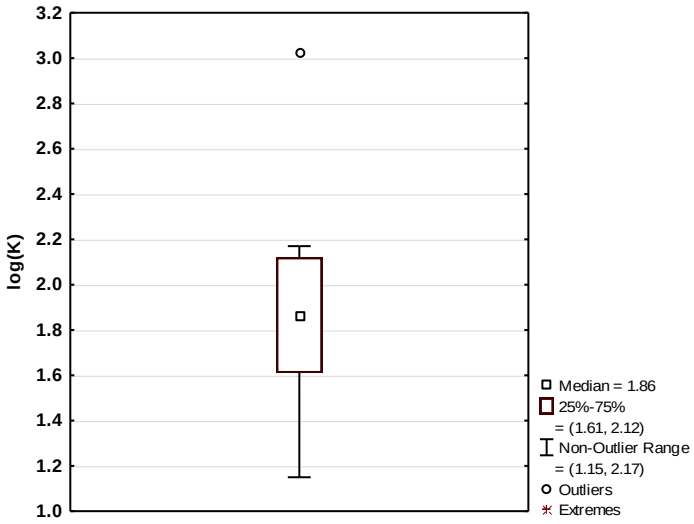

Figure 3: Box-Whiskers plot of log(K) D_1 values [39]

We can see that the larger value of log(K) is shown as being an outlier. This effect is due only to the lacking of experimental data in the abovementioned interval. Figure 4 shows the histogram of frequencies for log(K) D_5 data.

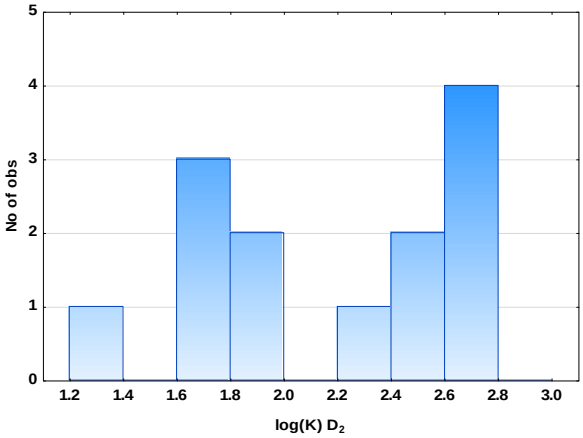

Figure 4: Histogram of frequencies for log(K) D_5 data

In this case we can see that the data is more homogeneous in the sense that no large empty intervals exist. Figure 5 shows the Box-Whiskers plot of log(K) D_5 values with median and quartile values.

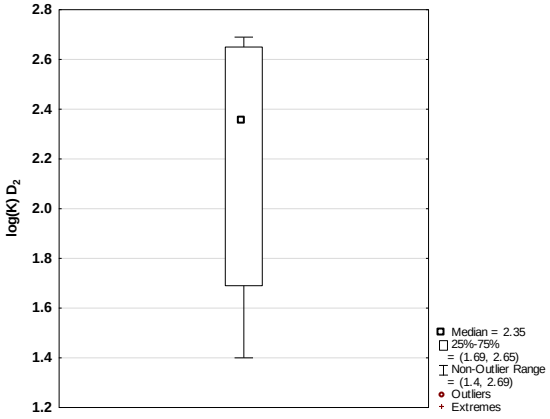

Figure 5: Box-Whiskers plot of log(K) D_5 values

In this case no outliers or extremes appear in the plot.

Calculations

The electronic structure of all molecules was calculated within the Density Functional Theory at the B3LYP/6-31g(d,p) level with full geometry optimization [40]. The Gaussian 16software was employed [41]. All the data needed to calculate the numerical values for the local atomic reactivity indices was obtained from the Gaussian results with the D-Cent-QSAR software [42]. All the electron populations smaller than or equal to 0.01e were considered as being zero. Negative MO electron populations and MO populations greater than 2 coming from Mulliken Population Analysis were corrected [43]. Since the resolution of the system of linear equations is not possible because we have not sufficient molecules, we made use of Linear Multiple Regression Analysis (LMRA) techniques to find the best solution. For each case, a matrix containing the dependent variable (log(K) in this case) and the local atomic reactivity indices of all atoms of the common skeleton as independent variables was built. The Statistica software was used [39].

Now, let us consider the following problem. We are dealing with a group of molecules, some with different number of atoms and some with substituents placed at different places. On the other hand, Eq. 1 must have the same number of atoms in the system of equations. To satisfy this mandatory condition, the logical way to proceed is to select atoms having an equivalent one in all the molecules. The chemical nature of the equivalent atoms does not need to be the same (for example, in one molecule the atom is carbon while in another molecule it can be nitrogen). This set of atoms is called the common skeleton and it is hypothesized that it accounts for almost all the interactions leading to the expression of a given biological activity. It is more or less obvious that this skeleton could have different sizes. The common skeleton for this case is shown in Fig. 6.

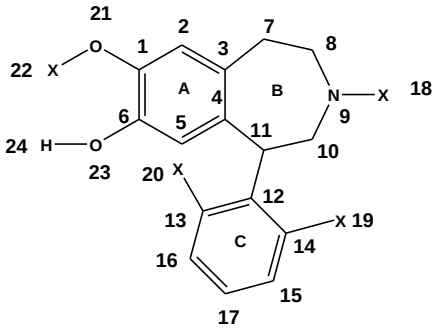

Figure 6: Common skeleton of 1-phenylbenzazepines derivatives

Results

Results for D_1 receptor binding affinity

The best equation obtained is:

$$\log(K)=2.55+0.29S_{17}^{N}(LUMO+2)^{*}-20.00F_{8}(LUMO+2)^{*}-0.44\mu_{18}^{*}+0.55\mu_{8}^{*} \quad (2)$$

with n=13, adj-R^2=0.96, F(4,8)=64.692 ($p<0.00000$) and SD=0.10. No outliers were detected and no residuals fall outside the $\pm 2\sigma$ limits. Here, $S_{17}^{N}(LUMO+2)^{*}$ is the nucleophilic superdelocalizability of the third lowest empty local MO of atom 17, $F_8(LUMO+2)^{*}$ is the electron population of the third lowest empty local MO of atom 8, μ_{18}^{*} is the local atomic electronic potential of atom 18 and μ_8^{*} is the local atomic electronic potential of atom8 [17]. Tables 2 and 3 show the beta coefficients, the results of the t-test for significance of coefficients and the matrix of squared correlation coefficients for the variables of Eq. 2. There are no significant internal correlations between independent variables (Table 3). Figure 7 displays the plot of observed *vs.* calculated values.

Table 2: Beta coefficients and t-test for significance of coefficients in Eq. 2

Var.	Beta	t(8)	p-level
$\mathbf{S_{17}^{N}(LUMO+2)^{*}}$	0.74	11.56	0.000003
$\mathbf{F_8(LUMO+2)^{*}}$	-0.58	-8.92	0.00002
$\boldsymbol{\mu_{18}^{*}}$	-0.32	-5.09	0.0009
$\boldsymbol{\mu_{8}^{*}}$	0.26	3.96	0.004

Table 3: Matrix of squared correlation coefficients for the variables in Eq. 2

	S_{17}^{N}(LUMO+2)*	F_8(LUMO+2)*	μ_{18}^{*}	μ_{8}^{*}
S_{17}^{N}(LUMO+2)*	1.00			
F_8(LUMO+2)*	0.00	1.00		
μ_{18}^{*}	0.03	0.03	1.00	
μ_{8}^{*}	0.05	0.07	0.01	1.00

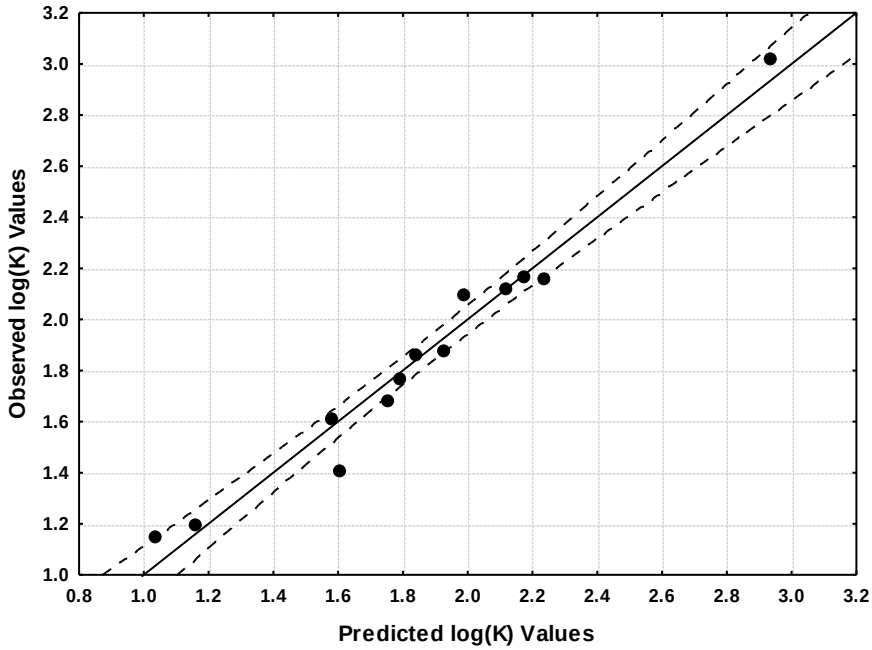

Figure 7: Plot of predicted vs. observed log(K) values (Eq. 2). Dashed lines denote the 95% confidence interval

The associated statistical parameters of Eq. 2 indicate that this equation is statistically significant and that the variation of the numerical values of a group of four local atomic reactivity indices of atoms constituting the common skeleton explains about 96% of the variation of the numerical values of log(K). Figure 7, spanning about 2 orders of magnitude, shows that there is a good correlation of observed *versus* calculated values. Figures 8, 9 and 10 show, respectively, the plot of predicted values vs. residuals scores, the plot of residual vs. deleted residuals and the normal probability plot of residuals.

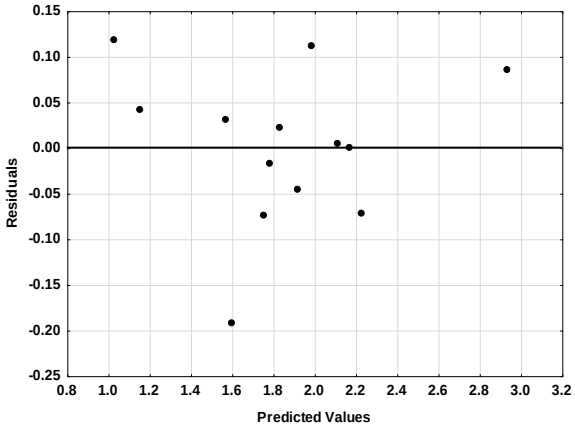

Figure 8: Plot of predicted values vs. residuals scores

The plot shows no indication of any kind of ordering. Then this plot supports the idea that the linear equation is a good first approach to study these molecular systems.

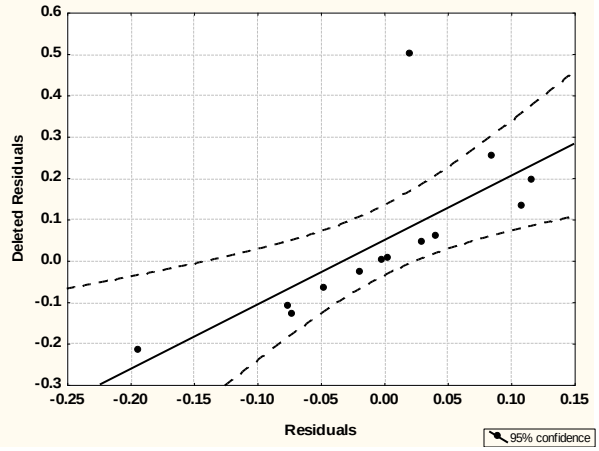

Figure 9: Plot of residual vs. deleted residuals

In this case we have one point localized very far from the confidence interval, strongly suggesting that this molecule has one or more interactions with the binding site through atoms not belonging to the common skeleton. This point deserves further research.

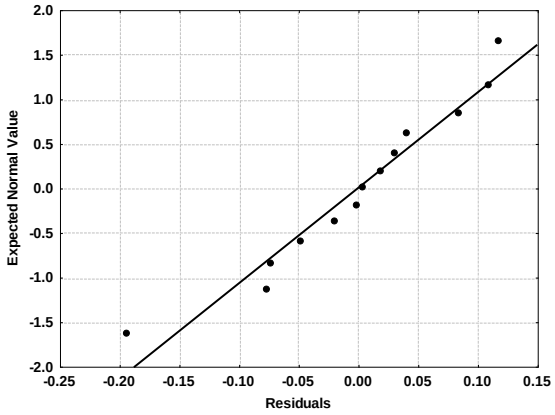

Figure 10: Normal probability plot of residuals

These three plots show that the linear equation 2 is a good starting point for a QSAR analysis.

Results for D_5 receptor binding affinity

The best equation obtained is:

$$\log(K)=2.64-21.80F_8(\text{LUMO+2})^*+2.09Q_{18}^{*max}-2.06F_1(\text{LUMO+2})^* \quad (3)$$

with n=13, adj-R^2=0.91, F(3,9)=44.038 ($p<0.00001$) and SD=0.14. No outliers were detected and no residuals fall outside the ±2σ limits. Here, F_8(LUMO+2)* is the electron population of the third lowest empty local MO of atom 8, Q_{18}^{*max} is the maximal amount of charge atom 18 may receive and F_1(LUMO+2)* is the electron population of the third lowest empty local MO of atom 1. Tables 4 and 5 show the beta coefficients, the results of the t-test for significance of coefficients and the matrix of squared correlation coefficients for the variables of Eq. 3. There are no significant internal correlations between independent variables (Table 5). Figure 11 displays the plot of observed *vs.* calculated values.

Table 4: Beta coefficients and t-test for significance of coefficients in Eq. 3

Var.	Beta	t(9)	p-level
F_8(LUMO+2)*	-21.80	-7.63	0.00003
Q_{18}^{*max}	2.09	4.39	0.002
F_1(LUMO+2)*	-2.06	-3.68	0.005

Table 5: Matrix of squared correlation coefficients for the variables in Eq. 3

	F_8(LUMO+2)*	Q_{18}^{*max}	F_1(LUMO+2)*
F_8(LUMO+2)*	1.00		
Q_{18}^{*max}	0.02	1.00	
F_1(LUMO+2)*	0.00	0.20	1.00

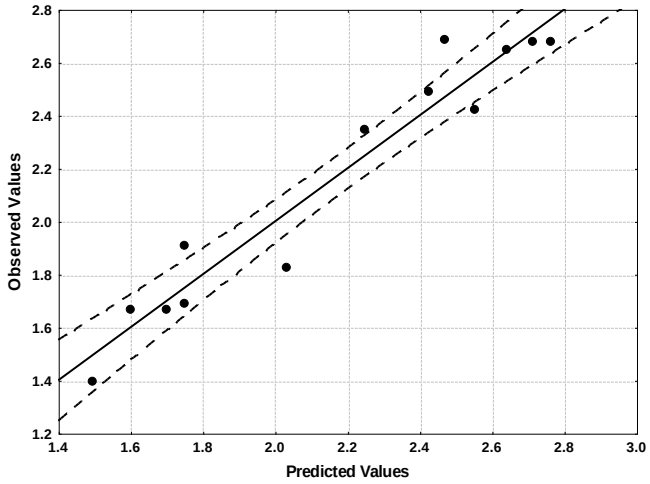

Figure 11: Plot of predicted vs. observed log(K) values (Eq. 3). Dashed lines denote the 95% confidence interval

The associated statistical parameters of Eq. 3 indicate that this equation is statistically significant and that the variation of the numerical values of a group of three local atomic reactivity indices of atoms constituting the common skeleton explains about 91% of the variation of log(K). Figure 11, spanning about 1.2 orders of magnitude, shows that there is a relatively good correlation of observed *versus* calculated values. Figures 12, 13 and 14 show, respectively, the plot of predicted values vs. residuals scores, the plot of residual vs. deleted residuals and the normal probability plot of residuals.

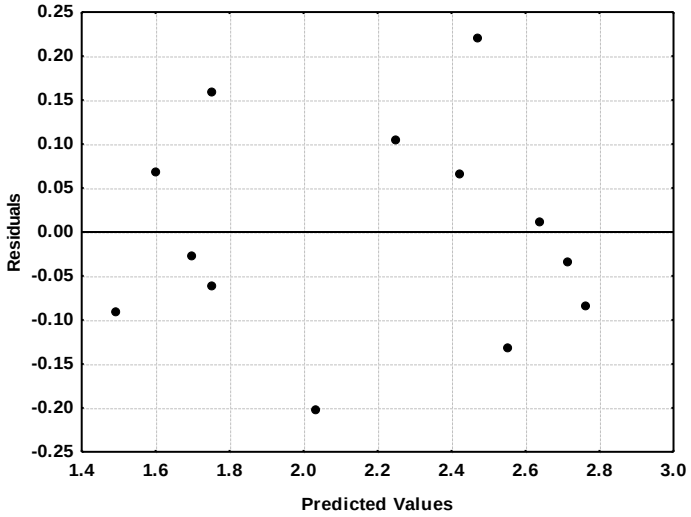

Figure 12: Plot of predicted values vs. residuals scores

No indication of a pattern is observed.

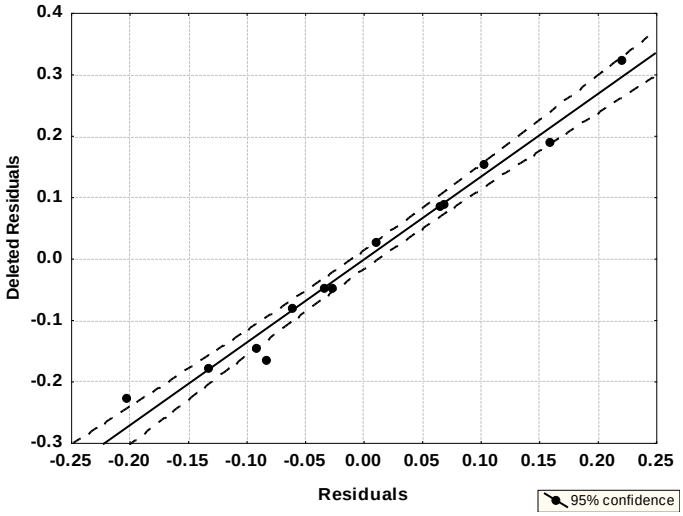

Figure 13: Plot of residual vs. deleted residuals

Almost all points are inside the confidence interval or very close to it.

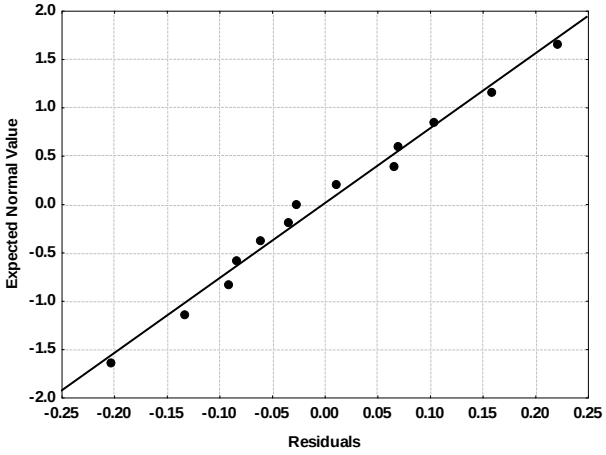

Figure 14: Normal probability plot of residuals

These three plots are a clear support to the hypothesis stating that linear Eq. 3 is a reliable tool to use for the analysis.

Local Molecular Orbitals

Table 6 shows the local MO structure of atoms 1, 8, 17 and 18 (see Fig. 6). Nomenclature: Molecule (HOMO)/ (HOMO-2)*(HOMO-1)*(HOMO)*- (LUMO)* (LUMO+1)* (LUMO+2)*.

Table 6: The local MO structure of atoms 1, 8, 17 and 18

Mol.	Atom 1	Atom 8	Atom 17	Atom 18
1 (72)	70π71π72π- 74π75π76π	70σ71σ72σ- 76σ81σ83σ	69π70π71π- 73π74π76π	62σ67σ71σ- 77σ78σ79σ
2 (80)	74π78π80π- 83π84π85π	75σ79σ80σ- 84σ87σ88σ	77π78π79π- 81π82π84π	68σ69σ79σ- 86σ 87σ88σ
3 (88)	81σ86π88π- 91π92π93π	83σ87σ88σ- 93σ96σ98σ	84π85π86π- 89π90π91σ	75σ76σ87σ- 95σ96σ97σ
4 (89)	84π87π89π- 92π93π94π	86σ88σ89σ- 96σ97σ99σ	86π87π88π- 90π91π93σ	76σ78σ88σ- 95σ96σ97σ
5 (85)	80π83π85π- 88π90π91σ	82σ84σ85σ- 90σ94σ95σ	82π83π84π- 86π87π89σ	73σ75σ84σ- 91σ92σ93σ

6 (84)	82π83π84π- 87π88π89π	82σ83σ84σ- 88σ94σ96σ	81π82π83π- 85π86π88π	73σ77σ83σ- 91σ94σ98σ
7 (92)	90π91π92π- 95π96π97π	90σ91σ92σ- 97σ102σ103σ	88π89π90π- 93π94π95σ	80σ85σ91σ- 100σ102σ107σ
8 (93)	91π92π93π- 96π97π98π	88σ92σ93σ- 97σ103σ104σ	89π90π91π- 94π95π97σ	82σ85σ92σ- 100σ103σ105σ
9 (91)	89π90π91π- 94π95π96π	89σ90σ91σ- 95σ96σ102σ	87π88π89π- 92π93π96π	86σ90σ91σ- 95σ100σ102σ
10 (99)	97π98π99π- 102π103π104π	94σ98σ99σ- 103σ105σ106σ	95π96π97π- 100π101π10σ	91σ94σ98σ- 103σ104σ108σ
11 (100)	94π98π99π- 103π104π105π	98σ99σ100σ- 104σ106σ107σ	96π97π98π- 101π102π10σ	92σ95σ100σ- 105σ109σ111σ
12 (89)	87π88π89π- 92π93π94π	87σ88σ89σ- 93σ94σ99σ	85π86π87π- 90π91π93σ	79σ81σ89σ- 97σ102σ104σ
13 (96)	90π94π95π- 99π100π101π	94σ95σ96σ- 100σ102σ103σ	92π93π94π- 97π98π100σ	88σ91σ96σ- 101σ106σ107σ

Discussion

Molecular Electrostatic Potential (MEP)

Molecular Electrostatic Potential (MEP) maps allow determining which sectors of the molecule are nucleophiles or electrophiles. Also, they enable us to visualize the charge-related properties of molecules at a certain distance of the nuclei, and they are useful for detecting the similitudes and differences in the MEPs and provide a first idea about how the molecules approach the site. Here we present the MEP maps of the most and less active molecules for each one of the receptors, calculated at 4.5Å of the nuclei [44].

In the case of D1 receptor, figures 15 and 16 show, respectively, the MEP map of molecules 6 (the most active) and 10 (the less active) calculated at 4.5 Å of the nuclei.

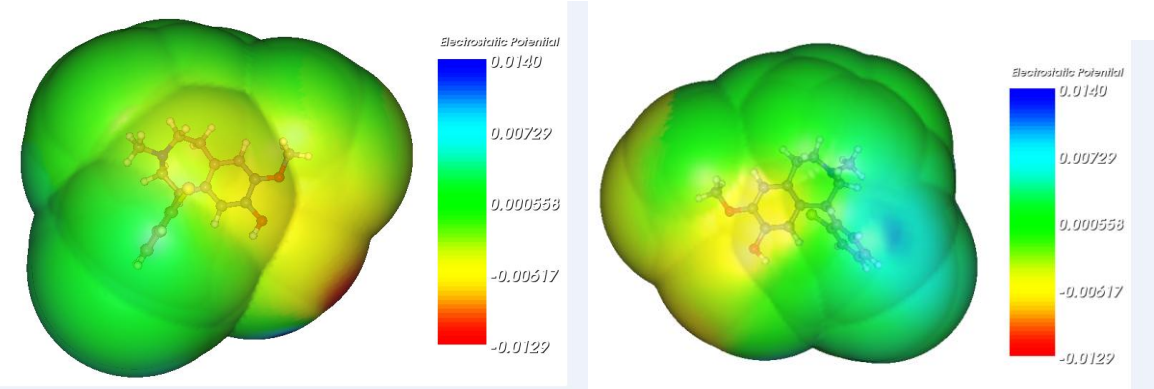

Figure 15: MEP map of molecule 6 (left and right are rotated views)

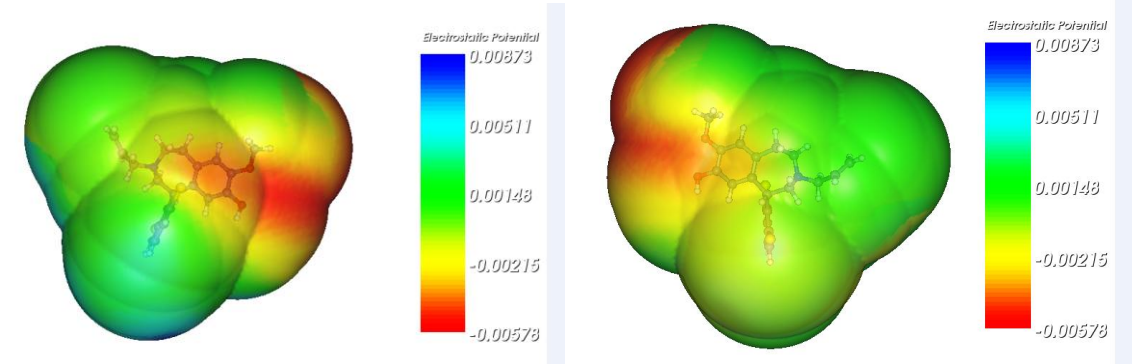

Figure 16: MEP map of molecule 10 (left and right are rotated views)

In the case of D_5 receptor figures 17 and 18 show, respectively, the MEP map of molecules 3 (left, the most active) and 11 (right, the less active) calculated at 4.5 Å of the nuclei.

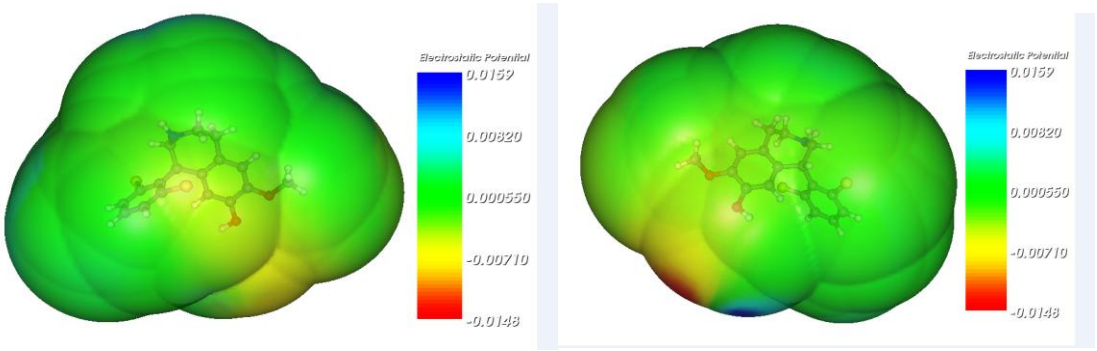

Figure 17: MEP map of molecule 3 (left and right are rotated views)

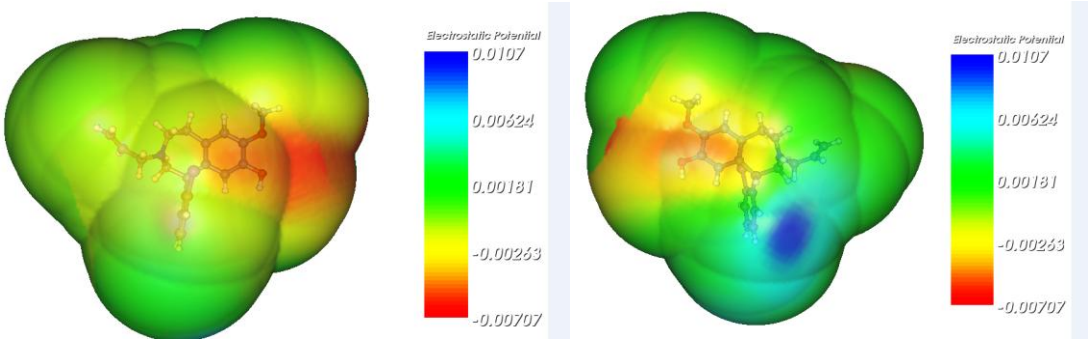

Figure 18: MEP map of molecule 11 (left and right are rotated views)

We can see that there are some differences in the MEP maps for the four molecules, but they are not enough significant allowing suggesting a structure-activity relationship.

Figure 19 shows the MEP maps of molecules 6 and 10 [45].

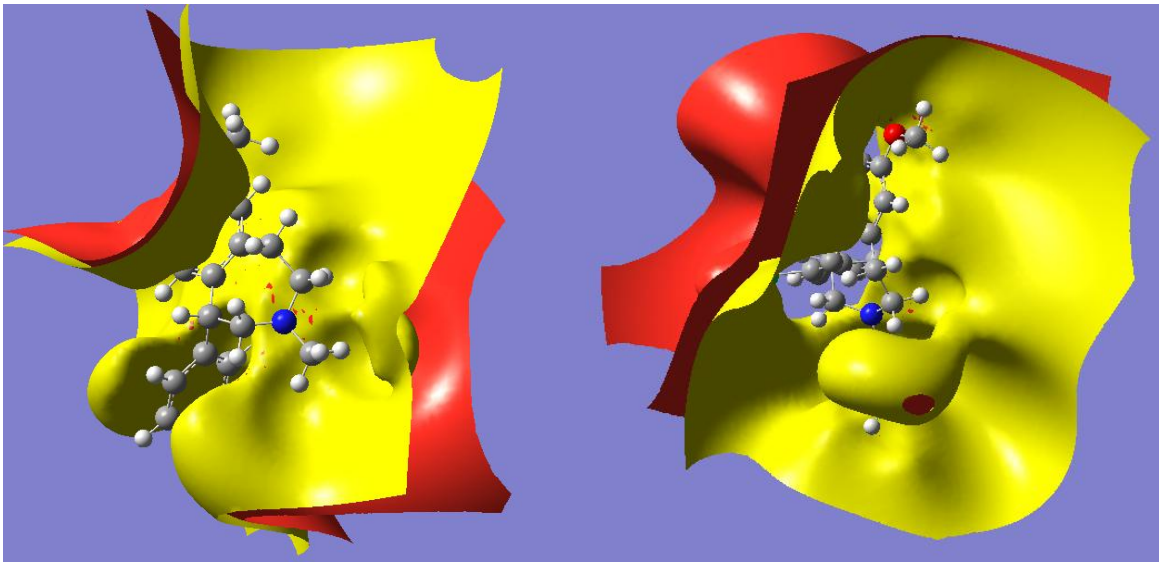

Figure 19: MEP of molecules 6 (left) and 10 (right). The red surface corresponds to negative MEP values (-0.0004) and the yellow surface to positive MEP values (0.0004).

Figure 20 shows the MEP maps of molecules 3 and 11.

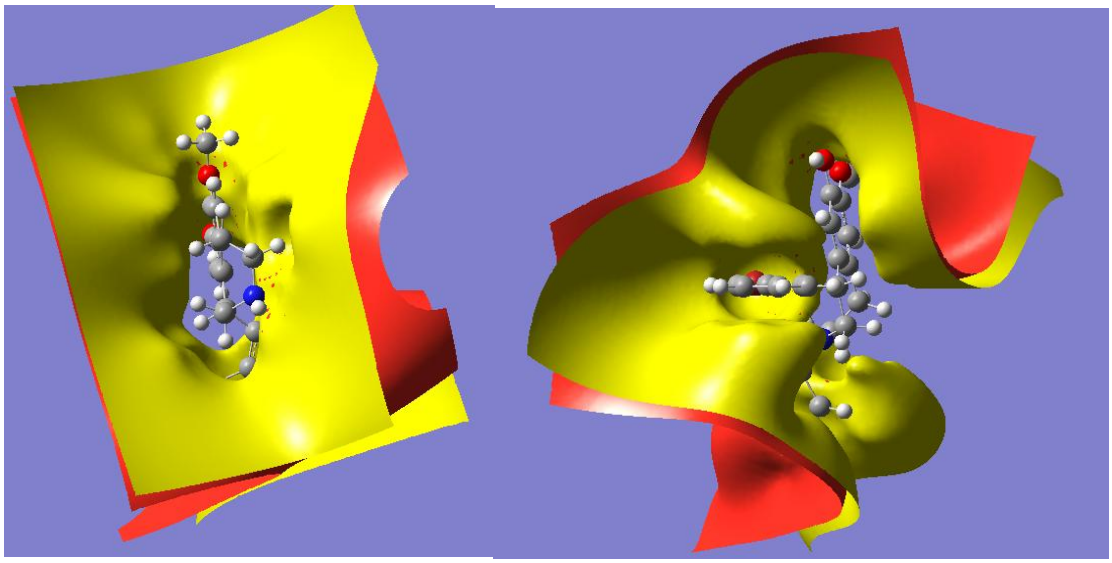

Figure 20: MEP of molecules 3 (left) and 11 (right). The red surface corresponds to negative MEP values (-0.0004) and the yellow surface to positive MEP values (0.0004).

In these figures we may appreciate several differences in the MEP maps. At short distances the map's structure is strongly influenced by the kind of substituents but it is only possible to state some generalizations such as the possibility of an H-bond, a pi-pi interaction, etc.

Discussion of the results for D_1 receptor binding affinity [46, 47]

Table 2 shows that the importance of variables in Eq. 2 is S_{17}^{N}(LUMO+2)*> F_8(LUMO+2)*> μ_{18}^{*}> μ_{8}^{*}.A high D_1 receptor affinity is associated with low numerical values for S_{17}^{N}(LUMO+2)*, large numerical values for F_8(LUMO+2)*, small (negative) values for μ_{18}^{*} and large (negative) numerical values for μ_{8}^{*}. The atoms appearing in Eq. 2 are shown in figure 21.

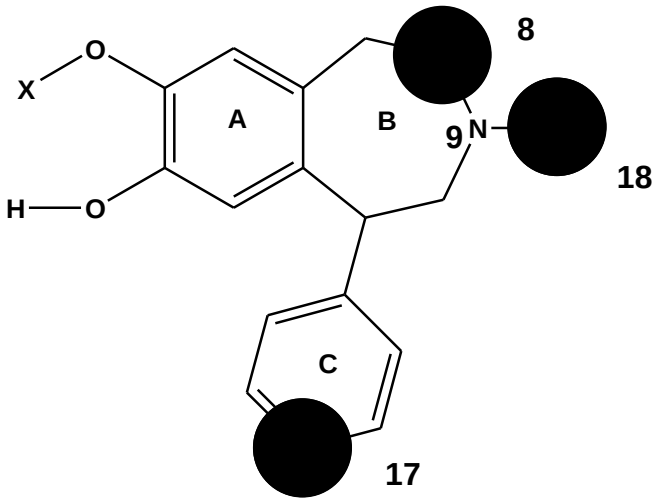

Figure 21: Atoms appearing in Eq. 2.

Atom 8 is a sp^3 carbon atom in ring B (Fig. 6). Two local atomic reactivity indices belonging to this atom appear in Eq. 2: F_8(LUMO+2)* and μ_8^{*}.All local MOs have a sigma nature. Large numerical values for F_8(LUMO+2)* are associated with a higher receptor affinity. The only way to obtain these values is by increasing the electron population on it, i.e., by limiting the localization of this MO to atom 8. This will make this local MO more prone to interact with electron-rich centers or with anions. On the other hand, larger (negative) numerical values for μ_8^{*} are also associated with high receptor affinity. Knowing that μ_8^{*} is the midpoint between the local $(HOMO)_8^{*}$ energy

and the local $(LUMO)_8^*$ energy, the only way to get these large negative values is by lowering the $(LUMO)_8^*$ energy or by lowering the $(HOMO)_8^*$ energy (or by both procedures carried out at the same time). In the first case we obtain a more reactive $(LUMO)_8$* and in the other a less reactive $(HOMO)_8^*$. $(HOMO)_8^*$ coincides with the molecular HOMO. $(LUMO)_8$* coincides with empty molecular MOs other than LUMO in all cases. These two local atomic reactivity indices are coincident when we think that atom 8 should be interacting with an electron-rich center or with an anion. The most probable interactions are the alkyl ones. Atom 18 is the first atom of the substituent bonded to N9 (H or C, see Table 1 and Fig. 6).Table 6 shows that all local MO have a sigma nature. Small (negative) values for μ_{18}^* are associated with high receptor affinity. These values can be obtained by shifting upwards the $(HOMO)_{18}^*$ and/or the $(LUMO)_{18}^*$ energies. In the first case we have a better electron donor and in the second a bad electron acceptor. If we consider the hydrogen atom, the interaction with the site could be through a N9-H18…X (X= N, O) hydrogen bond. When X18 is carbon (sp^3 in all cases) it is possible to suggest alkyl interactions. It seems that it is not possible to suggest a common interaction site for H and C. Atom 17 is a sp^2 carbon atom in ring C (Fig. 6). Table 6 shows that the local (LUMO)* coincides with the molecular LUMO in all cases and that the local (HOMO)* coincides with molecular orbitals close to the molecular HOMO in all cases. Low numerical values for S_{17}^N(LUMO+2)* are associated with high receptor affinity. These values can be obtained by shifting upwards the energies of $(LUMO+2)_{17}^*$ making this MO less reactive. Applying the rule we established earlier, $(LUMO+1)_{17}^*$ and $(LUMO)_{17}^*$ energies should be also shifted upwards, making atom 17 a bad electron acceptor. Therefore, it is possible to suggest that atom 17 will be prone to interact with electron-deficient sites or with cations. Table 6 shows that the three highest occupied local MOs have a pi nature. Therefore possible interactions of atom 17 are π-cation, π-π, and/or π-alkyl [46, 47]. All the suggestions are displayed in the partial 2D pharmacophore of Fig. 22.

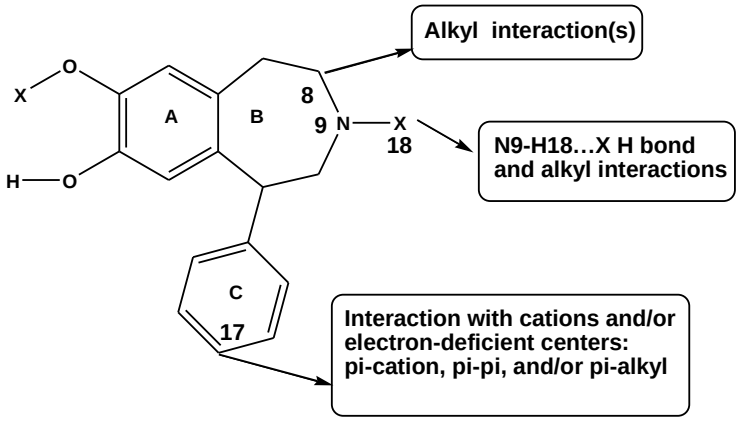

Figure 22: Partial 2D pharmacophore (D_1)

Discussion of the results for D_5 receptor binding affinity

Table 4 shows that the importance of variables in Eq. 3 is F_8(LUMO+2)*>> Q_{18}^{*max}> F_1(LUMO+2)*. The atoms appearing in Eq. 3 are shown in figure 23.

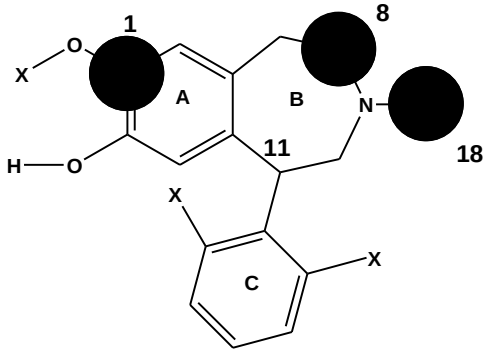

Figure 23: Atoms appearing in Eq. 3

A high D_5 receptor affinity is associated with large numerical values for F_8(LUMO+2)*, small numerical values for Q_{18}^{*max} and large numerical values for F_1(LUMO+2)*.Atom 8 is a sp^3 carbon in ring B. As high receptor affinities are associated with large numerical values for F_8(LUMO+2)* like in the D_1 results, all what was mentioned above applies here. Atom 18 is the first atom of the substituent bonded to N9 (H or C, see Table 1 and Fig. 6). A high D_5 receptor affinity is associated with small numerical values for Q_{18}^{*max}. This requirement indicates that atom 18 should not be a good charge acceptor and we may enhance this effect by shifting upwards the $(LUMO)_{18}^*$ energy. Like the previous case, we cannot find a common interaction site for H and C atoms. If the H atoms are bad electron acceptors we may suggest a strong N9…H18…X (X= N, O) hydrogen bond. In the case of a C18 atom we can suggest alkyl interactions. A possible strategy to deal with this problem is to do an analysis with molecules in which X18 all substituents have more than one atom in order to enlarge the common skeleton. This requires a larger number of molecules. Atom 1 is a sp^2 carbon in ring A (see Fig. 6). Larger numerical values for F_1(LUMO+2)* are associated with a higher D_5 receptor affinity. Table 6 shows that the three highest occupied and the three lowest empty local MOs have a pi nature. Larger numerical values for F_1(LUMO+2)* are obtained is by increasing the electron population on it, i.e., by limiting the localization of this MO to atom 1. This will make this local MO more prone to interact with electron-rich centers or with anions. Using the rules stated about the appearance of MOs other that the frontier ones we suggest that $(LUMO+1)_1$* and $(LUMO)_1$* must also increase their reactivity. Therefore, atom 1 could be involved in π-anion, π-π and/or π-alkyl interactions [46, 47]. All the suggestions are displayed in the partial 2D pharmacophore of Fig. 24.

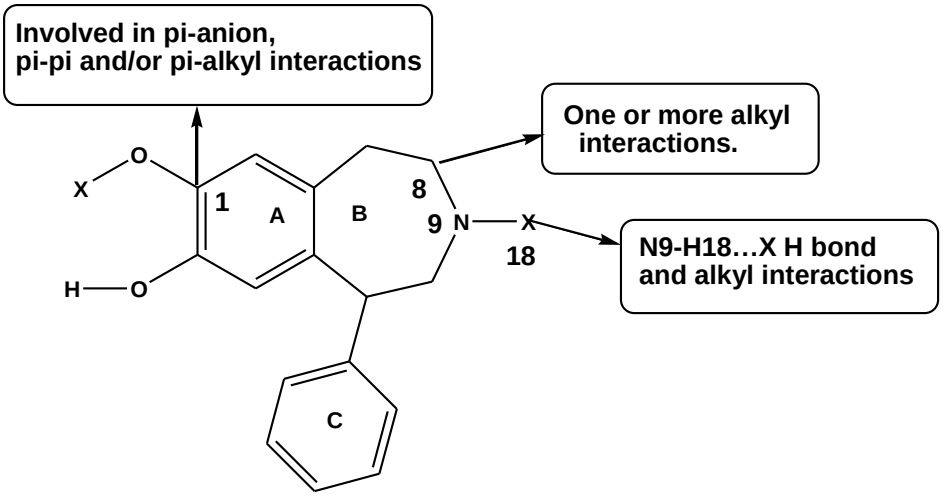

Figure 24: Partial 2D pharmacophore (D_5)

In summary, for series of 1-phenylbenzazepines we have obtained statistically significant relationships between the electronic structure and dopamine D_1 and D_5 receptor affinities. For the atoms appearing to be involved in the drug-receptor interaction we have suggested possible interactions that could be tested by experimentalists.

References

[1]. Mishra, A.; Singh, S.; Shukla, S. Physiological and Functional Basis of Dopamine Receptors and Their Role in Neurogenesis: Possible Implication for Parkinson's disease. *Journal of experimental neuroscience* **2018,** 12, 1179069518779829-1179069518779829.

[2]. Gómez-Jeria, J. S.; Ojeda-Vergara, M. Electrostatic medium effects and formal quantum structure-activity relationships in apomorphines interacting with D_1 and D_2 dopamine receptors. *International Journal of Quantum Chemistry* **1997,** 61, 997-1002.

[3]. Gómez-Jeria, J. S.; Valdebenito-Gamboa, J. Electronic structure and docking studies of the Dopamine D_3 receptor binding affinity of a series of [4-(4-Carboxamidobutyl)]-1-arylpiperazines. *Der Pharma Chemica* **2015,** 7, 323-347.

[4]. Gómez-Jeria, J. S.; Valdebenito-Gamboa, J. A Density Functional Study of the Relationships between Electronic Structure and Dopamine D_2 receptor binding affinity of a series of [4-(4-Carboxamidobutyl)]-1-arylpiperazines. *Research Journal of Pharmaceutical, Biological and Chemical Sciences* **2015,** 6, 203-218.

[5]. Gautier, K. S.; Kpotin, G. A.; Mensah, J.-B.; Gómez-Jeria, J. S. Quantum-Chemical Study of the Relationships between Electronic Structure and the Affinity of Benzisothiazolylpiperazine Derivatives for the Dopamine Hd2l and Hd3 Receptors. *The Pharmaceutical and Chemical Journal* **2019,** 6, 73-90.

[6]. Gómez-Jeria, J. S.; Garrido-Sáez, N. A DFT analysis of the relationships between electronic structure and affinity for dopamine D_2, D_3 and D_4 receptor subtypes in a group of 77-LH-28-1 derivatives. *Chemistry Research Journal* **2019,** 4, 30-42.

[7]. Gómez-Jeria, J. S.; López-Aravena, R. A Theoretical Analysis of the Relationships between Electronic Structure and Dopamine D_4 Receptor Affinity in a series of compounds based on the classical D_4 agonist A-412997. *Chemistry Research Journal* **2020,** 5, 1-9.

[8]. Gómez-Jeria, J. S.; Ibertti-Arancibia, A. A DFT study of the relationships between electronic structure and dopamine D_1 and D_2 receptor affinity of a group of (S)-enantiomers of 11-(1,6-dimethyl-1,2,3,6-tetrahydropyridin-4-yl)-5*H*-dibenzo[b,e][1,4]diazepines. *Chemistry Research Journal* **2021,** 6, 116-131.

[9]. Giri, R.; Namballa, H. K.; Sarker, A.; Alberts, I.; Harding, W. W. Synthesis and dopamine receptor pharmacological evaluations on ring C ortho halogenated 1-phenylbenzazepines. *Bioorganic & Medicinal Chemistry Letters* **2020,** 30, 127305-127305.

[10]. Gómez Jeria, J. S. La Pharmacologie Quantique. *Bollettino Chimico Farmaceutico* **1982,** 121, 619-625.

[11]. Gómez-Jeria, J. S.; Espinoza, L. Quantum-chemical studies on acetylcholinesterasa inhibition. I. Carbamates. *Journal of the Chilean Chemical Society* **1982,** 27, 142-144.

[12]. Gómez-Jeria, J. S. On some problems in quantum pharmacology I. The partition functions. *International Journal of Quantum Chemistry* **1983,** 23, 1969-1972.

[13]. Gómez-Jeria, J. S. Modeling the Drug-Receptor Interaction in Quantum Pharmacology. In *Molecules in Physics, Chemistry, and Biology*, Maruani, J., Ed. Springer Netherlands: 1989; Vol. 4, pp 215-231.

[14]. Gómez-Jeria, J. S.; Ojeda-Vergara, M. Parametrization of the orientational effects in the drug-receptor interaction. *Journal of the Chilean Chemical Society* **2003,** 48, 119-124.

[15]. Barahona-Urbina, C.; Nuñez-Gonzalez, S.; Gómez-Jeria, J. S. Model-based quantum-chemical study of the uptake of some polychlorinated pollutant compounds by Zucchini subspecies. *Journal of the Chilean Chemical Society* **2012,** 57, 1497-1503.

[16]. Alarcón, D. A.; Gatica-Díaz, F.; Gómez-Jeria, J. S. Modeling the relationships between molecular structure and inhibition of virus-induced cytopathic efects. Anti-HIV and anti-H1N1 (Influenza) activities as examples. *Journal of the Chilean Chemical Society* **2013,** 58, 1651-1659.

[17]. Gómez-Jeria, J. S. *Elements of Molecular Electronic Pharmacology (in Spanish)*. 1st ed.; Ediciones Sokar: Santiago de Chile, 2013; p 104.

[18]. Gómez-Jeria, J. S. A New Set of Local Reactivity Indices within the Hartree-Fock-Roothaan and Density Functional Theory Frameworks. *Canadian Chemical Transactions* **2013,** 1, 25-55.

[19]. Gómez-Jeria, J. S.; Flores-Catalán, M. Quantum-chemical modeling of the relationships between molecular structure and in vitro multi-step, multimechanistic drug effects. HIV-1 replication inhibition and inhibition of cell proliferation as examples. *Canadian Chemical Transactions* **2013,** 1, 215-237.

[20]. Paz de la Vega, A.; Alarcón, D. A.; Gómez-Jeria, J. S. Quantum Chemical Study of the Relationships between Electronic Structure and Pharmacokinetic Profile, Inhibitory Strength toward Hepatitis C virus NS5B Polymerase and HCV replicons of indole-based compounds. *Journal of the Chilean Chemical Society* **2013,** 58, 1842-1851.

[21]. Gómez-Jeria, J. S. 45 Years of the KPG Method: A Tribute to Federico Peradejordi. *Journal of Computational Methods in Molecular Design* **2017,** 7, 17-37.

[22]. Gómez-Jeria, J. S.; Morales-Lagos, D. The mode of binding of phenylalkylamines to the Serotonergic Receptor. In *QSAR in design of Bioactive Drugs*, Kuchar, M., Ed. Prous, J.R.: Barcelona, Spain, 1984; pp 145-173.

[23]. Gómez-Jeria, J. S.; Morales-Lagos, D. R. Quantum chemical approach to the relationship between molecular structure and serotonin receptor binding affinity. *Journal of Pharmaceutical Sciences* **1984,** 73, 1725-1728.

[24]. Gómez-Jeria, J. S.; Morales-Lagos, D.; Rodriguez-Gatica, J. I.; Saavedra-Aguilar, J. C. Quantum-chemical study of the relation between electronic structure and pA2 in a series of 5-substituted tryptamines. *International Journal of Quantum Chemistry* **1985,** 28, 421-428.

[25]. Gómez-Jeria, J. S.; Morales-Lagos, D.; Cassels, B. K.; Saavedra-Aguilar, J. C. Electronic structure and serotonin receptor binding affinity of 7-substituted tryptamines. *Quantitative Structure-Activity Relationships* **1986,** 5, 153-157.

[26]. Gómez-Jeria, J. S.; Cassels, B. K.; Saavedra-Aguilar, J. C. A quantum-chemical and experimental study of the hallucinogen (±)-1-(2,5-dimethoxy-4-nitrophenyl)-2-aminopropane (DON). *European Journal of Medicinal Chemistry* **1987,** 22, 433-437.

[27]. Gómez-Jeria, J. S.; Ojeda-Vergara, M.; Donoso-Espinoza, C. Quantum-chemical Structure-Activity Relationships in carbamate insecticides. *Molecular Engineering* **1995,** 5, 391-401.

[28]. Gómez-Jeria, J. S.; Lagos-Arancibia, L. Quantum-chemical structure-affinity studies on kynurenic acid derivatives as Gly/NMDA receptor ligands. *International Journal of Quantum Chemistry* **1999,** 71, 505-511.

[29]. Gómez-Jeria, J. S.; Lagos-Arancibia, L.; Sobarzo-Sánchez, E. Theoretical study of the opioid receptor selectivity of some 7-arylidenenaltrexones. *Boletin de la Sociedad Chilena de Quimica* **2003,** 48, 61-66.

[30]. Gómez-Jeria, J. S. A DFT study of the relationships between electronic structure and peripheral benzodiazepine receptor affinity in a group of N,N-dialkyl-2- phenylindol-3-ylglyoxylamides (Erratum in: J. Chil. Chem. Soc., 55, 4, IX, 2010). *Journal of the Chilean Chemical Society* **2010,** 55, 381-384.

[31]. Gómez-Jeria, J. S. A theoretical study of the relationships between electronic structure and anti-inflammatory and anti-cancer activities of a series of 6,7-substituted-5,8-quinolinequinones. *International Research Journal of Pure and Applied Chemistry* **2014,** 4, 270-291.

[32]. Gómez-Jeria, J. S. A Preliminary Formal Quantitative Structure-Activity Relationship Study of some 1,7-Bis-(amino alkyl)diazachrysene Derivatives as Inhibitors of Botulinum Neurotoxin Serotype A Light Chain and Three P. falciparum Malaria Strains. *Journal of Computational Methods in Molecular Design* **2014,** 4, 32-44.

[33]. Gómez-Jeria, J. S. A Theoretical Study of the Relationships between Electronic Structure and Antifungal Activity against *Botrytis cinerea* and *Colletotrichum lagenarium* of a Group of Carabrone Hydrazone Derivatives. *Research Journal of Pharmaceutical, Biological and Chemical Sciences* **2015,** 6, 688-697.

[34]. Gómez-Jeria, J. S.; Castro-Latorre, P. A Density Functional Theory analysis of the relationships between the Badger index measuring carcinogenicity and the electronic structure of a series of substituted Benz[a]anthracene derivatives. *Chemistry Research Journal* **2017,** 2, 112-126.

[35]. Gómez-Jeria, J. S.; Moreno-Rojas, C. Dissecting the drug-receptor interaction with the Klopman-Peradejordi-Gómez (KPG) method. I. The interaction of 2,5-dimethoxyphenethylamines and their N-2-methoxybenzyl-substituted analogs with 5-HT_{1A} serotonine receptors. *Chemistry Research Journal* **2017,** 2, 27-41.

[36]. Kpotin, G.; Gómez-Jeria, J. S. Quantum-Chemical Study of the Relationships between Electronic Structure and Anti-Proliferative Activities of Quinoxaline Derivatives on the K562 and MCF-7 Cell Lines. *Chemistry Research Journal* **2018,** 3, 20-33.

[37]. Gómez-Jeria, J. S.; Valenzuela-Hueichaqueo, N. J. The relationships between electronic structure and human A_1 adenosine receptor binding affinity in a series of triazolopyridine derivatives. *Chemistry Research Journal* **2020,** 5, 226-236.

[38]. Gómez-Jeria, J. S.; Crisóstomo-Cáceres, S. R.; Robles-Navarro, A. On the compatibility between formal QSAR results and docking results: the relationship between electronic structure and H5N1 (A/goose/Guangdong/SH7/2013) neuraminidase inhibition by some Tamiflu derivatives as an example. *Chemistry Research Journal* **2021,** 6, 46-59.
[39]. Statsoft. *Statistica v. 8.0*, 2300 East 14 th St. Tulsa, OK 74104, USA, 1984-2007.
[40]. The results presented here are obtained from what is now a routinary procedure. For this reason, all papers have a similar general structure. This model contains *standard* phrases for the presentation of the methods, calculations and results because they do not need to be rewritten repeatedly and because the number of possible variations to use is finite. See: Hall, S., Moskovitz, C., and Pemberton, M. 2021. Understanding Text Recycling: A Guide for Researchers. Text Recycling Research Project. Online at textrecycling.org. In.
[41]. Frisch, M. J.; Trucks, G. W.; Schlegel, H. B.; Scuseria, G. E.; Robb, M. A.; Cheeseman, J. R.; Scalmani, G.; Barone, V.; Petersson, G. A.; Nakatsuji, H.; Li, X.; Caricato, M.; Marenich, A. V.; Bloino, J.; Janesko, B. G.; Gomperts, R.; Mennucci, B.; Hratchian, H. P. *Gaussian 16 16Rev. A.03*, Gaussian: Pittsburgh, PA, USA, 2016.
[42]. Gómez-Jeria, J. S. *D-Cent-QSAR: A program to generate Local Atomic Reactivity Indices from Gaussian16 log files*, v. 1.0; Santiago, Chile, 2020.
[43]. Gómez-Jeria, J. S. An empirical way to correct some drawbacks of Mulliken Population Analysis (Erratum in: J. Chil. Chem. Soc., 55, 4, IX, 2010). *Journal of the Chilean Chemical Society* **2009,** 54, 482-485.
[44]. Varetto, U. *Molekel 5.4.0.8*, Swiss National Supercomputing Centre: Lugano, Switzerland, 2008.
[45]. Dennington, R. D.; Keith, T. A.; Millam, J. M. *GaussViev 5.0.8*, GaussViev 5.0.8, 340 Quinnipiac St., Bldg. 40, Wallingford, CT 06492, USA, 2000-2008.
[46]. Gómez-Jeria, J. S.; Robles-Navarro, A.; Kpotin, G.; Garrido-Sáez, N.; Gatica-Díaz, N. Some remarks about the relationships between the common skeleton concept within the Klopman-Peradejordi-Gómez QSAR method and the weak molecule-site interactions. *Chemistry Research Journal* **2020,** 5, 32-52.
[47]. Gómez-Jeria, J. S.; Kpotin, G. Some Remarks on The Interpretation of The Local Atomic Reactivity Indices Within the Klopman-Peradejordi-Gómez (KPG) Method. I. Theoretical Analysis. *Research Journal of Pharmaceutical, Biological and Chemical Sciences* **2018,** 9, 550-561.